

Sudden changes in nitrogen dioxide emissions over Greece due to lockdown after the outbreak of COVID-19

Maria-Elissavet Koukouli^{1*}, Ioanna Skoulidou¹, Andreas Karavias², Isaak Parcharidis², Dimitris Balis¹, Astrid Manders³, Arjo Segers³, Henk Eskes⁴ and Jos van Geffen⁴

¹ Laboratory of Atmospheric Physics, Aristotle University of Thessaloniki, Greece.

² Department of Geography, Harokopio University, Athens, Greece.

³ TNO, Climate, Air and Sustainability, Utrecht, The Netherlands.

⁴ Royal Netherlands Meteorological Institute (KNMI), De Bilt, The Netherlands.

* Correspondence: mariliza@auth.gr

Abstract: The unprecedented order, in modern peaceful times, for near-total lockdown of the Greek population, as means of protection against the Severe Acute Respiratory Syndrome CoronaVirus-2, commonly known as COVID-19, infection, has brought unintentional positive side-effects to the country's air quality levels. S5P/TROPOMI monthly mean tropospheric nitrogen dioxide (NO₂) observations show an average change of -34% to +20% [-39% to -5%] with an average decrease of -15% [-11%] for March and April 2020 respectively, compared to the previous year, over the six larger Greek metropolitan areas, attributable mostly to vehicular emission reductions. For the capital city of Athens, weekly analysis was statistically possible for the S5P/TROPOMI observations which revealed a marked decline in NO₂ load between -8% and -43% for seven of the eight weeks studied, in agreement to the equivalent OMI/Aura observations as well as the ground-based estimates of a Multi-Axis Differential Optical Absorption Spectroscopy ground-based instrument. Chemical transport modelling of the NO₂ columns, provided by the LOTOS-EUROS Chemical Transport Model, shows that the magnitude of these reductions cannot solely be attributed to the difference in meteorological factors affecting NO₂ levels during March and April 2020 and the equivalent time periods of the previous year. Taking this factor into account, the resulting decline was estimated to range between ~ -25% and -65% for the five of the eight weeks studied, with the remaining three weeks showing a positive average of ~ 10% which is postulated to the uncertainty of this methodology which is based on differences. As a result this analysis, we conclude that the effect of the COVID-19 lockdown and restriction in transport emissions over Greece is ~ -10%. As transport is the second largest, after the industrial, sector, that affects Greece's air quality, this occasion may well help policy makers in enforcing more targeted measures to aid Greece in further reducing emissions according to international air quality standards.

Keywords: Air quality; nitrogen dioxide; NO_x; emissions; Sentinel-5P; TROPOMI; LOTOS-EUROS; COVID-19; pandemic; Athens; Greece

1. Introduction

In this work we aim to quantify the decline in tropospheric nitrogen dioxide (NO₂) levels over Greece during the ongoing Severe Acute Respiratory Syndrome CoronaVirus-2, commonly known as COVID-19, pandemic, as sensed by the space-borne S5P/TROPOMI, hereafter TROPOMI, instrument. By comparing the relative levels for the months of March and April for years 2020 and 2019, while properly accounting for the differences in meteorology using the simulations of a Chemical Transport Model, CTM, we quantify the improvement in local and regional air quality due to the reduced nitrogen oxides (NO_x) emissions.

In the following sections, we provide basic information on tropospheric NO_x, we focus on current knowledge of the nominal NO_x emissions over Greece, we then present a brief overview of the capabilities of current and past satellite instruments in sensing abrupt atmospheric content changes and furthermore provide the dates when the different lockdown measures were enforced nationwide in Greece.

1.1. Nitrogen oxides in the troposphere

Nitrogen dioxide (NO₂) and nitrogen oxide (NO), referred to more commonly as nitrogen oxides (NO_x), are important trace gases in the Earth's troposphere. NO_x are emitted as a result of both anthropogenic activities, such as fossil fuel combustion and biomass burning, and natural processes, such as microbiological processes in soils, wildfires and lightning. In the presence of sunlight, the photochemical cycle of tropospheric ozone (O₃) converts

49 NO into NO₂ on a timescale of minutes and so NO₂ is considered a robust measure for concentrations of nitrogen
50 oxides (Jacob, 1999). For typical levels of the OH radical, the lifetime of NO_x in the lower troposphere is less than
51 a day, normally a few hours depending on the season and the rates of the photochemical reactions [see for e.g.
52 Beirle et al., 2011; Mijling and van der A, 2012]. As a result, it is well accepted that NO₂ fluxes will remain relatively
53 close to their source which, first of all, makes it possible for NO_x emissions to be well detected from space [see for
54 e.g. Stavrakou et al., 2008; Lamsal et al., 2010; van der A et al., 2008] but also precludes any transboundary pollution
55 effects which might otherwise hinder this study.

56 In the troposphere, NO₂ plays a key role in air quality issues, as it directly affects human health [WHO, 2016].
57 In the European Union, the evidence of NO₂ health effects has led to the establishment of air quality standards for
58 the protection of human health. Limit values for NO₂ are set at 200 µg m⁻³ for 1 h average concentrations (with 18
59 exceedances permitted per year), and 40 µg m⁻³ for annual average concentrations (European Council Directive
60 2008/50/EC, 2008). Concentrations above the annual limit value for NO₂ are still widely registered across Europe,
61 even if concentrations and exposures continue to decrease [EEA, 2019]. In Greece in particular, the annual average
62 standard of 40 µg m⁻³ has not been exceeded between years 2007 and 2017 when assuming all in situ stations; the
63 traffic stations of Athens and Thessaloniki however show annual levels up to 45 µg m⁻³ for years 2015 to 2017. It
64 hence follows logically that monitoring closely abrupt changes in NO_x emissions for diverse locations plays a key
65 role in shaping future environmental policies and directives.

66 1.2. Nitrogen dioxide emissions over Greece

67 According to the EEA Report No 8/2019, updated by the EU 2019 Environmental Implementation Review for
68 Greece [EU, 2019], the country's NO_x emissions by sector originate from road transport, industry (which mainly
69 covers the energy production and distribution sector), non-road transport, household and agriculture. The relative
70 percentages for NO_x air emissions, separated by sector, as extracted from the 2018 Air Emission Account 2015
71 report by the Hellenic Statistical Authority [HAS, 2017], are: industry 48%, transport 22%, energy supply 18%,
72 manufacturing 6%, central heating 4%, agriculture 1% and others 1%. Based on the European Environmental
73 Agency, EEA, European Pollutant Release and Transfer Register, 77% of the reported industrial NO_x/NO₂
74 emissions over Greece came from thermal power stations and other combustion installations. The monthly energy
75 balance reports, composed by the Independent Power Transmission Operator of the Hellenic Electricity
76 Transmission System (IPTO, 2020), show that the total energy requested for March 2020 [4.152GWh] was lower by
77 -2.1% than 2019 [4.224GWh] , whereas for April 2020 [3.527GWh] was -9.8% lower than 2019 [3.527]. These
78 reductions are quite typical of the seasonality of the energy consumption in Greece which peaks in December and
79 January, due to heating needs, and in July and August, due to cooling needs, with seasonal lows in spring (April
80 and May) and autumn (October and November). Furthermore, in Fameli and Asimakopoulos, 2016, it is reported
81 that the annual mean NO_x emissions for Greece for years 2006 to 2012 can be attributed as follows, in order of
82 relevance: industry, 45±3%, road transport, 35±8%, shipping 11±3%, non-road transport, 10±4%, central heating,
83 5±2%, with agriculture and aviation showing an average of around 1± each. If we assume that years 2019 and 2020
84 were not exceptional in their temperature levels for the spring months, then it follows that changes in central
85 heating emissions will not be a significant part of the emission changes observed.

86 1.3. Sensing abrupt emission changes from space-borne sensors

87 Abrupt emission changes have already been reported using space-borne observations for a number of recent
88 local and continental circumstances. Castellanos and Boersma, 2012, reported significant reductions in nitrogen
89 oxides over Europe driven by environmental policy and the economic recession based on OMI/Aura observations
90 between 2004 and 2010. Vrekoussis et al., 2013 and Zyrichidou et al., 2019, report strong correlations between
91 pollutant levels and economic indicators showing that the 2008 economic recession has resulted in proportionally
92 lower levels of pollutants in large parts of Greece. The latter, for years 2008 to 2015, showed surprisingly that, while
93 the wintertime tropospheric NO₂ trends were negative, significant positive formaldehyde trends were observed
94 from space, shown to be due to increased usage of affordable indoor heating methods (e.g. fireplaces and wood
95 stoves). Space-sensed reductions in emissions, on a shorter time scale, have also been attributed to strict measures
96 enforced for benign reasons. Mijling et al., 2009, calculated, using OMI/Aura and CTM results, reductions in NO₂
97 concentrations of approximately 60% above Beijing during the 2008 Olympic and Paralympic Games. Ding et al.,

98 2015, showed a ~30% decrease in OMI/Aura columns, which was translated into a ~25% in actual emission levels
99 during the Nanjing 2014 Youth Olympic Games.

100 Numerous first reports suggesting an improved air quality in after the COVID-19 lockdown was enforced
101 have already been seen in major media outlets. Here we note the findings of Liu et al., 2020, who report for China,
102 based on both OMI/Aura and TROPOMI, a 48% drop in tropospheric NO₂ from the 20 days averaged before the
103 2020 Lunar New Year to the 20 days after, which is 20% larger than that from recent years, and relate the increase
104 in decline to the date of each Chinese province lockdown. Similar levels of tropospheric NO₂ decrease over different
105 Chinese provinces are reported by Ding et al., 2020 and Miyazaki et al., 2020. Bauwens et al., 2020, based on the
106 same sensors, also report an average NO₂ column drop over all Chinese cities of -40% relative to the same period
107 in 2019, while the decreases in Western Europe and the U.S. were found to range between -20 to -38%. Goldberg et
108 al., 2020, analyzed TROPOMI observations around large U.S. cities focusing on the effect of meteorological factors
109 and report that meteorological variations between years 2019 and 2020 can cause columnar NO₂ differences of ~15%
110 over monthly timescales. Compensating for meteorology, they then calculated a decrease in NO₂ levels between
111 9.2% and 43.4% among 20 cities in North America, with a median of 21.6%. Cersosimo et al., 2020, regrided the
112 TROPOMI observations down to the 1x1km level and found that the reductions measured by air quality in situ
113 measurements in the Po Valley, Italy, were very well reproduced by the satellite observations, while comparisons
114 over less polluted regions in the South of Italy provide mixed results, which may also be attributed to the lower
115 space-sensed levels. Virghileanu et al., 2020, also analysed the lockdown effect on Europe-wide pollution and
116 report correlations to in situ observations ranging between 0.5 and 0.75, while also demonstrating the usefulness
117 of such high spatial resolution satellite observations when used in tandem to other economic factors.

118 1.4. The COVID-19 situation over Greece

119 A short review on the COVID-19 situation over Greece is given here, mainly focusing on providing the dates
120 in March 2020 of the successive restrictive measures that affected NO_x emissions which were placed nationwide.
121 The country's General Secretariat for Civil Protection reacted quickly to the emerging situation in the neighbouring
122 country Italy and long before the first casualties were reported, major festivities for the Carnival season planned
123 for the 28th of February to the 2nd of March were cancelled, followed by cancellation of all other cultural and sporting
124 activities on March 8th. On the 11th of March, all levels of education were suspended, when also a first wave of
125 workplace closures begun and culminated on Monday 16th when all restaurants, coffee shops with sitting facilities,
126 and in general the food [apart from supermarkets] and hospitality industry were shut down. In the following two
127 days, all remaining retail activities were suspended apart from pharmacies. On Monday 16th restrictions on the size
128 of public gatherings were announced and the public transport section [buses, trams, underground, trains] started
129 to reduce capacity. On Monday 23rd of March, full restrictions on the people's movements were imposed with strict
130 stay-at-home mandates, with exceptions for essential working personnel, including all religious-related
131 congregations, with a complete and without exception restriction around the Greek Orthodox Easter holidays of
132 the 19th of April. The country remained in full lockdown mode until May 4th. We should note here that most
133 industrial activities continued normal operations, albeit with a skeleton crew, which might account for some of the
134 higher load observed around the city of Athens where most of these activities are located.

135 2. Materials and Methods

136 In this section we introduce the TROPOMI tropospheric NO₂ observations, the CTM LOTOS-EUROS
137 simulations and the proposed methodology to account for the different meteorological conditions between the
138 nominal period of March-April 2019 and the disrupted one of March-April 2020.

139 2.1. TROPOMI NO₂ observations.

140 The recently launched TROPOMI instrument on the Sentinel-5 Precursor (S5P) mission [Veefkind et al., 2012]
141 has been providing global atmospheric observations since early 2018. Its very high spatial resolution of 3.5 × 7 km²,
142 upgraded to 3.5 × 5.5 km² in August 2019, and improved signal-to-noise ratio compared to previous space-borne
143 instruments, permits the detection of tropospheric pollution from small-scale emission sources and the estimation
144 of very localized emissions from anthropogenic activities, such as industrial point sources, as well as regional fires.

145 Lorente et al., 2019, have already reported updated emissions over the Paris metropolitan area using TROPOMI
146 observations, while Ialongo et al., 2020, have assessed the capabilities of this instrument in evaluating city-wide air
147 quality levels compared to the more traditional ground-based and in situ NO₂ monitoring methods.

148 In this work we use the publicly available TROPOMI offline v1.2 and v1.3 for March–April 2019 and for March–
149 April 2020 tropospheric NO₂ data accessed via the Copernicus Open Data Access Hub. The algorithm producing
150 this data is described by van Geffen et al. (2019) and is based on the approach used for processing OMI/Aura NO₂
151 data within DOMINO and the FP7 Quality Assurance for Essential Climate Variables, projects (Boersma et al, 2011;
152 2018). Routine validation is being carried out by the Validation Data Analysis Facility, who also provide the
153 Validation Report of the Copernicus Sentinel-5 Precursor Operational Data Products quarterly. The S5P
154 tropospheric NO₂ columns are routinely compared to ground-based column data at 19 ground-based Multi-Axis
155 Differential Optical Absorption Spectroscopy, MAXDOAS, stations. The latest report reports a negative bias of
156 typically -22% to -37% for clean and slightly polluted conditions, reaching values of -51% over highly polluted
157 areas (ROCVR #08, 2020). Furthermore, within ROCVR #08, the case of Athens was used as an example of the
158 lockdown effects on NO₂ observations from both ground and space. It is shown that both the Athens MAXDOAS
159 instrument (operated by the Institute of Environmental Physics, University of Bremen) and the S5P observations
160 observe a significant drop in NO₂ levels between March 3rd and March 13th, in line to the first nation-wide measures
161 on March 10th, 2020, with further restrictions on later days (closure of business, ban on non-essential movement,
162 see [https://www.bloomberg.com/news/articles/2020-04-17/humbled-greeks-show-the-world-how-to-handle-the-
163 virus-outbreak.](https://www.bloomberg.com/news/articles/2020-04-17/humbled-greeks-show-the-world-how-to-handle-the-virus-outbreak)) NO₂ columns over Athens remained consistently low for weeks after, while the MAXDOAS
164 instrument overall is performing very well, with a mean difference to the TROPOMI observations of $1.40 \pm 3.50 \times 10^{15}$
165 molecules/cm² (median of 0.25×10^{15} molecules/cm²) for the 385 coincident days of observations between 01.05.2018
166 and 28.11.2020 (<https://mpc-vdaf-server.tropomi.eu/no2/no2-offl-maxdoas/athens>). We should note at this point
167 that since in this work the main findings refer to relative differences between different time periods will be
168 examined, absolute differences to standard instruments do not affect our findings, as the stability of the TROPOMI
169 datasets is assured.

170 For the purposes of this work, orbital files over Greece, between 19° and 30°E and 34° and 42°N, were gridded
171 onto a 0.10x0.05° grid for different temporal scenarios. The data have been filtered, as recommended, using the
172 quality flag indicator ≥ 75 assuring the data under this flag is restricted to cloud-free (cloud radiance fraction < 0.5)
173 and snow-ice free observations. An example figure is presented in Section 3.1 (Figure 1) where the major NO_x
174 emitting sectors around Greece are prominent, the capital city Athens and the second largest city Thessaloniki, in
175 the North, as well as emissions by one of the two largest thermal power plants, in Ptolemaida, also in the North
176 and an important thermal power plant in Northern Macedonia, near the Greek border, where such trans-border
177 pollution transport is often visible. The domain also includes major emissions from known locations in the Turkish
178 Asia Minor coast, both originating from cities and major power plant activities, as well as the major shipping track
179 that emerges from the Strait of Bosphorus in Istanbul moving SW towards Athens before turning Westwards
180 towards the Mediterranean Sea.

181 2.2. LOTOS-EUROS CTM simulations.

182 The open source chemical transport model LOTOS—EUROS v2.2.001 is used for the purposes of this study to
183 simulate NO₂ columns over the Greek domain for March and April for years 2019 and 2020. The CTM model,
184 <https://lotos-euros.tno.nl/>, is originally aimed at air pollution studies and simulates gases (O₃, NO_x, SO₂, etc) as
185 well as aerosols (sulfate, nitrate, PM₁₀, PM_{2.5} etc.) in the troposphere. The gas-phase chemistry of the model is a
186 modified version of CBM-IV (Gery et al., 1989). The Isorropia II module (Fountoukis and Nenes, 2007) is used for
187 the aerosol chemistry, while detailed information on the model and its activity can be found in Manders et al., 2017.
188 LOTOS-EUROS is the national air quality model for the Netherlands (Vlemmix et al., 2015), and has been used for
189 specific studies as well to investigate NO₂ values (Timmermans et al., 2011; Curier et al., 2012; 2014). LOTOS-
190 EUROS also participates at the operational Copernicus Atmosphere Monitoring Service (CAMS) consisting one of
191 the seven CTMs that provide the official CAMS ensemble air quality forecasting service, while its capabilities were
192 demonstrated during the Monitoring Atmospheric Composition and Climate, MACC, and continued in the
193 MACC-II (Monitoring Atmospheric Composition and Climate: Interim Implementation) European projects
194 (Marécal et al., 2015). Vlemmix et al., 2015, compared LOTOS-EUROS NO₂ tropospheric columns with MAXDOAS,

195 measurements, and found a good agreement between the two datasets, with a correlation coefficient between the
196 daily averaged columns equal to 0.72. Schaap et al., 2013, compared the LOTOS-EUROS NO₂ simulations with
197 OMI/Aura retrievals and also showed that the model captures the NO₂ spatial distribution satisfactorily and is able
198 to explain 91% of the OMI signal variation across Europe, while the systematic difference was attributed to the
199 summer period.

200 In this work, LOTOS-EUROS NO₂ simulations over Greece as those presented and discussed thoroughly in
201 Skoulidou et al., 2020 are used. The model uses off-line meteorology extracted from the Operational Forecast Data
202 from the European Centre for Medium-range Weather Forecasts, ECMWF. These meteorological model level fields
203 cover temperature, boundary layer height, specific humidity, wind components, half level pressures, cloud
204 coverage, cloud liquid and ice water content, rain and snow water content, total cloud coverage, convective and
205 large-scale precipitation, wind components at 10 meters, etc. In addition, surface fields that include orography, soil
206 type, land/sea mask, sea surface and soil temperature, dew point temperature at 2 meters, surface latent and
207 sensible heat fluxes, surface solar downward radiation, and similar, are also included. The different level type
208 fields are obtained at a 3-hour temporal resolution while the surface fields are imported at a 1-hour resolution. The
209 horizontal resolution of the meteorological input fields is 7km×7km. In the vertical domain, the model
210 distinguishes 10 levels which extend from the surface to about 175hPa. The height of these levels refers to the levels
211 of the ECMWF meteorological input data that are further used to drive the model runs. The initial and boundary
212 conditions are constrained from a coarser run of LOTOS-EUROS that is performed over the larger European
213 domain (15° W to 45° E and 30° – 60° N) with a resolution of 0.25°×0.25°, as discussed in Skoulidou et al., 2020. The
214 anthropogenic emissions are provided by the CAMS-REG (CAMS Regional European emissions) inventory for the
215 year 2015 with a horizontal resolution of 0.1°×0.05° (Kuenen et al., 2014).

216 The LOTOS-EUROS NO₂ simulations over Greece reproduce very well the spatial variability of the TROPOMI
217 NO₂ columns over Greece, capturing the locations of low and high NO₂ columns (see their Figures 11 and 12 for
218 the summer and winter period respectively). The spatial correlation between the simulations over Athens
219 (Thessaloniki) and the TROPOMI observations is 0.95 (0.82) in summer and 0.82 (0.66) in winter, with a bias of
220 ±18% (+4 to -27%). Furthermore, comparisons to MAXDOAS systems located in both cities have shown that
221 LOTOS-EUROS simulates very well the diurnal variability of the NO₂, with biases between 0% and 30% depending
222 on the season for the overpass time of TROPOMI [around 12:00 UTC] quite in agreement to what was found in
223 Vlemmix et al., 2015 and Blechschmidt et al., 2020.

224 2.3. Comparative Methodology.

225 While it would make sense to simply compare the NO₂ levels over Greece for the two periods, assuming that
226 the emission sources have not changed dramatically between 2019 and 2020, one should not discard the effects that
227 various meteorological parameters have on NO₂ levels (Goldberg et al., 2020). Meteorological conditions, such as
228 wind speed, temperature inversions and the depth of the boundary layer, often play pivotal roles in local air quality
229 levels (Jacob and Winner, 2009). The ambient levels of secondary NO₂ pollution are determined through the
230 accumulation or dispersion of pollutants, low or high solar irradiances, regional transport of clear or polluted air
231 and atmospheric chemistry for the formation of secondary species, in this case via the chemical coupling of NO_x
232 with O₃ (for e.g. Seo et al., 2017).

233 To ensure that the observed decrease in NO₂ levels was not due to diverse meteorological conditions between
234 one year and the next, relative differences on NO₂ columns provided by the LOTOS-EUROS model are calculated
235 and their average magnitude is set as the expected contribution by the different meteorology. This forms a standard
236 level above which we expect COVID-19 related, i.e. emission-related, reductions. The premise of this thinking is as
237 follows: differences in the satellite observations will contain the intertwined effect of differences in meteorology
238 on concentrations and of differences in emissions. For the model we keep the emissions constant for the two periods
239 but use the meteorology of 2019 and 2020 so that we can isolate the impact of meteorology on concentrations. We
240 cannot of course exclude the possibility that the LOTOS-EUROS model has biases in the resulting NO₂ column
241 depending on the meteorological conditions. In Skoulidou et al., 2020, differences in night-time surface
242 concentrations between in situ observations and model simulations were found which were attributed to
243 modelling uncertainties in mixing under stable conditions. Within the methodology followed in this work we
244 expect any possible biases to cancel out in the difference fields calculated.

245 In this point we should stress that the satellite observations are more often than not gap-ridden, since in the
246 suggested screening all but nearly clear-skies remain. Spring-time months are rainy months, even for typically
247 sunny Greece, which means that a one-to-one comparison of the satellite observations for the two periods, even on
248 a weekly basis, is usually impossible. During our analysis it was found that, for e.g. the last week of March of 2020,
249 the first week of full lockdown, was fully cloudy for the Northern Greece even though the equivalent week in
250 March 2019 was all sunny. As a result, weekly comparisons were only possible for the major NO₂ hotspot over
251 Greece, the city of Athens, while the rest of the domain was examined on a monthly basis.

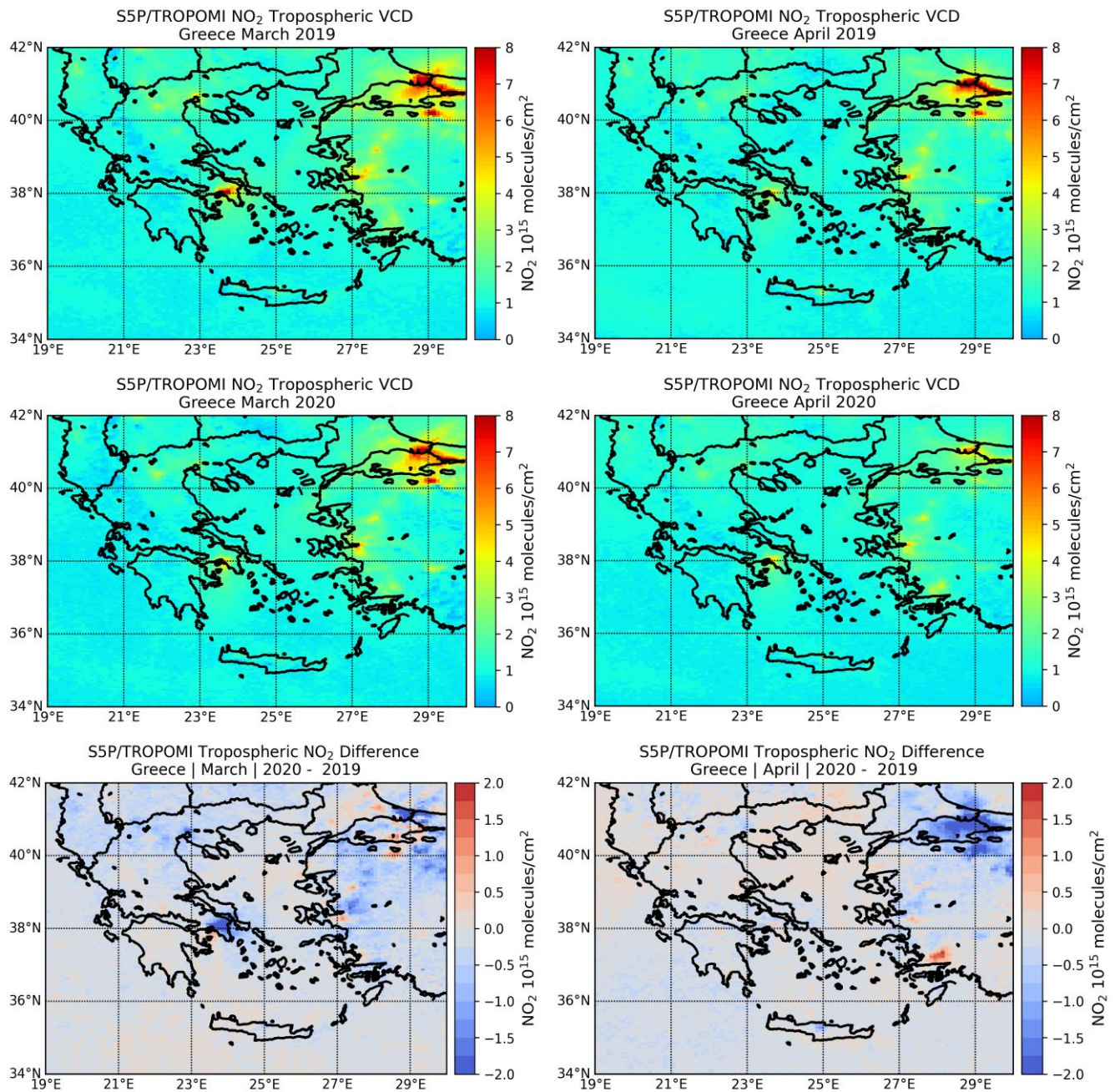
252 In technical terms, the LOTOS-EUROS simulations were performed on the entire timeline as discussed in
253 Section 2.2 but were restricted, on a daily basis, to the TROPOMI pixels that actually provided an observation when
254 performing the temporal averaging and producing the comparative plots. Even though a direct comparison of the
255 CTM results to the satellite data is not the focus of this paper, we imposed this filter to make sure that the same
256 days with the same meteorological conditions were viewed by both methods. Furthermore, as discussed in Eskes
257 and Boersma, 2003, so as to properly compare the modelled and measured columnar data, we applied the
258 TROPOMI averaging kernels, AKs, to the modelled profiles before extracting the CTM columns. The LOTOS-
259 EUROS CTM includes a module that imports the TROPOMI NO₂ orbital files in a pre-defined format, performs all
260 the necessary filtering, regridding and averaging of the datasets and executes the AK convolution of the nearest in
261 time observation to the CTM NO₂ simulated profile before outputting the profile and columnar information on the
262 predefined spatiotemporal grid.

263 3. Results

264 In the following section, we first show the effect on monthly NO₂ levels over the entire domain, the six Greek
265 cities with the largest number of inhabitants and we then present a more in depth analysis, on a weekly basis, for
266 the city of Athens, also examining the long term variability of tropospheric NO₂ levels over the capital city using
267 fifteen years of space-born observations by the Ozone Monitoring Instrument, OMI/Aura, as well as the air quality
268 *in situ* measurements of the Greek Ministry Environment & Energy network, reporting to the European
269 Environmental Agency.

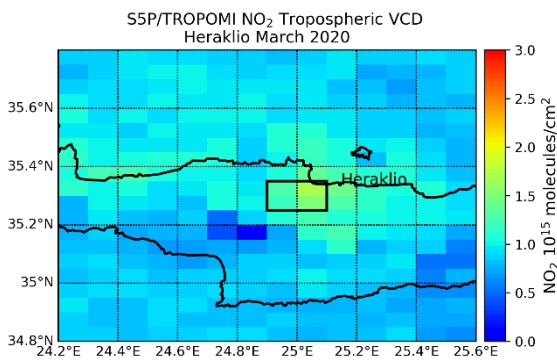
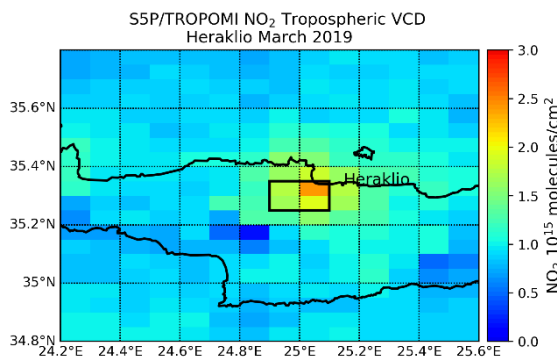
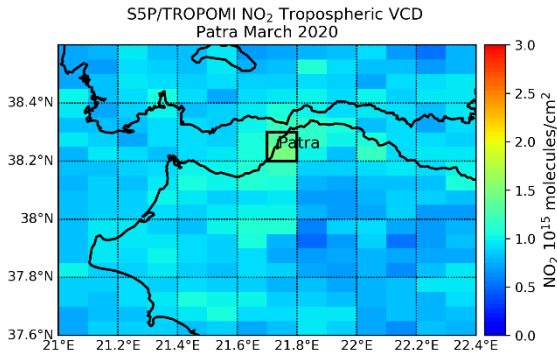
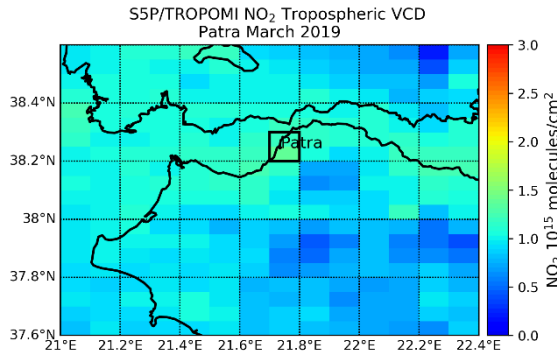
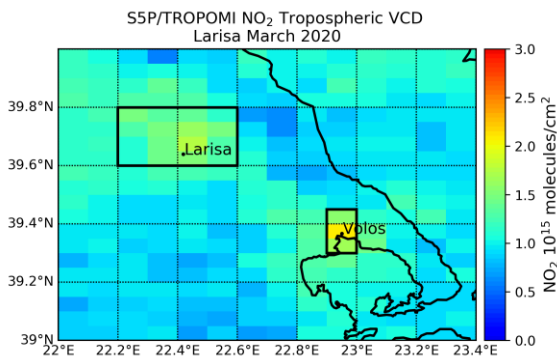
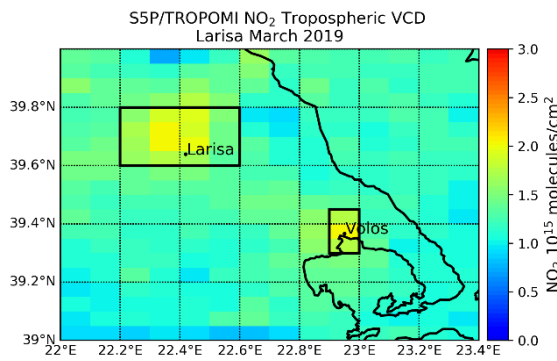
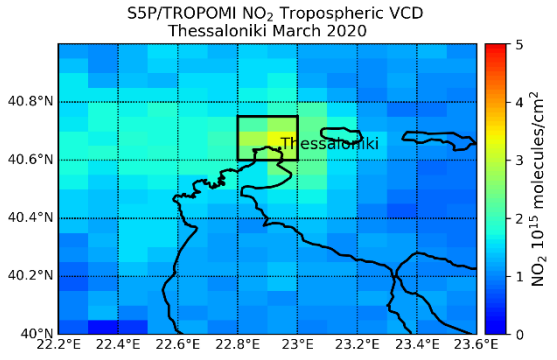
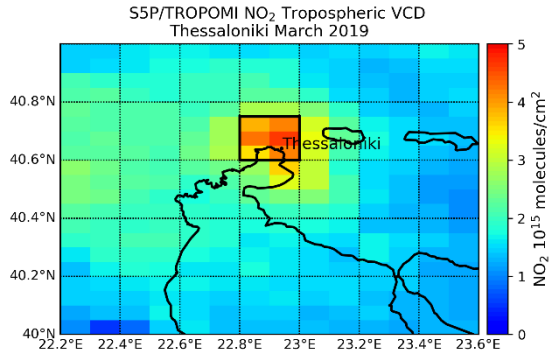
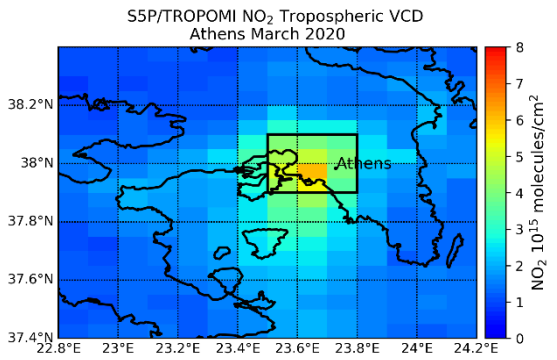
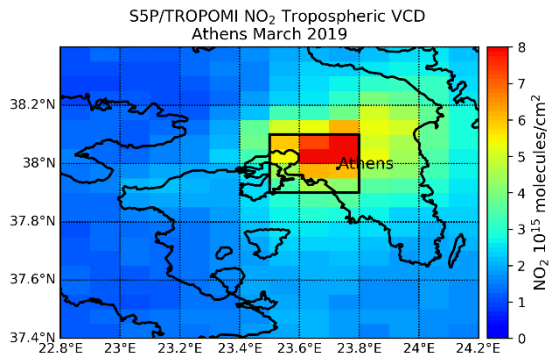
270 3.1. Lockdown effects on monthly NO₂ levels

271 In Figure 1 the monthly mean tropospheric NO₂ levels over Greece, the Northern neighboring countries, the
272 Aegean Sea as well as the coast of Turkey and the Istanbul area, are shown for year 2019 in the upper panel, year
273 2020 in the middle panel, their absolute difference in the lower panel, for the month of March in the left column
274 and the month of April in the right column. Even though the hotspots appear strong for year 2019, with discrete
275 shipping tracks and ground-tracks over Turkey showing clearly, the different meteorological conditions between
276 March and April obviously affect both the location of the maxima as well as the absolute level of those maxima.
277 Since Greece gradually entered full lockdown mode within the first three weeks of March, while Turkey imposed
278 intermittent movement restrictions from the beginning of April onwards, the NO₂ hotspot around the megacity of
279 Istanbul and the Bosphorus Strait is still pronounced in March 2020 [upper left] while in Greece most of the smaller
280 urban emission points are missing, and Athens is shown in sharp decline. In April 2020, the Turkish hotspots are
281 also reduced in magnitude, as expected. In the following sections we focus on specific hotspot locations and
282 introduce numerical findings.
283



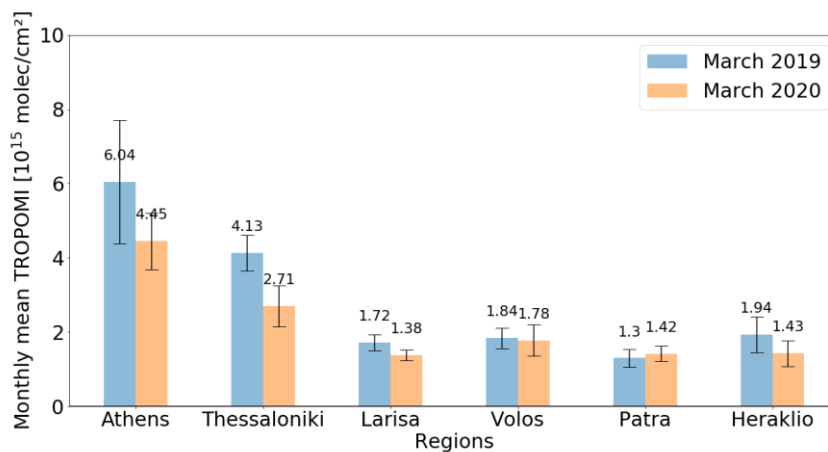
284 Figure 1 Monthly mean TROPOMI tropospheric NO₂ columns, in 10¹⁵ molecules/cm², for March [left] and April [right column]
 285 for the 2019 [top], 2020 [middle] and their absolute differences [lower panel].

286
 287 In Figure 2 the monthly mean TROPOMI tropospheric NO₂ columns, in 10¹⁵ molecules/cm², are depicted for
 288 March 2019 [left] and 2020 [right] for six major cities in Greece top to bottom, namely, Athens [37.98° N, 23.72° E],
 289 Thessaloniki [40.64° N, 22.94° E], Larisa [39.63° N, 22.41° E], Volos [39.36° N, 22.95° E], Patra [38.24° N, 21.73° E]
 290 and Heraklio [35.33° N, 25.14° E]. We focus on the locations where major transport emissions are expected
 291 since these six cities, according to the HAS, 2011, census, host 4.45 out of the 10.8 million of the Greek population
 292 (Table S1). Even though the NO₂ levels are low over the four smaller cities, we were interested in examining the
 293 ability of TROPOMI in sensing both the load and expected changes for these, relatively clean, cities [numeric results
 294 are given in Table 1]. The equivalent maps for April 2019 and 2020 are presented in Figure S1.
 295
 296



297 Figure 2. Monthly mean TROPOMI tropospheric NO₂ columns, in 10¹⁵ molecules/cm², for March 2019 [left] and March 2020 [right] for the five
 298 major cities in Greece. First row, Athens; second, Thessaloniki; third, Larisa and Volos; fourth, Patras and fifth, Heraklio. The boxes mark the
 299 pixels used in the numerical analysis.

300
 301 In Figure 3 the monthly mean TROPOMI tropospheric NO₂ columns, in 10¹⁵ molecules/cm², for March [upper]
 302 and April [lower] for the 2019 [blue] and 2020 [orange] are shown for the six major cities in Greece, from left to
 303 right, Athens, Thessaloniki, Larisa, Volos, Patra and Heraklio. Overall, the NO₂ levels are higher in all cases for
 304 both March months, than the equivalent April ones, and are proportional to the city population, with Athens and
 305 Thessaloniki showing the highest levels while the remaining four present similar NO₂ loading conditions. It is
 306 hence not surprising considering these rather low monthly mean reported satellite estimates, which approach the
 307 level of detectability of the satellite sensor that the changes vary widely from one location to the next and not
 308 always in the expected manner. We already note here that the associated standard deviation on the monthly mean
 309 levels for the four smaller cities is quite large, and might affect the robustness of findings later on in this work. In
 310 Table 1, the full statistics that relate to Figure 3 are given, where for the month of March, the relative differences in
 311 NO₂ loading sensed by the satellite sensor between 2019 and 2020 are shown to range from -3 to -34% in all cases
 312 except for the port city of Patra, where absolute changes of 0.12x10¹⁵ molecules/cm² result in percentage differences
 313 of +20%. Similarly, for the month of April, relative changes range from -39% to +5% however these mostly result
 314 from extremely small absolute changes of 0.06x10¹⁵ molecules/cm² (Athens) or 0.08x10¹⁵ molecules/cm² (Volos). The
 315 equivalent bar plot for the CTM tropospheric NO₂ columns is given in Figure S2, in the same format as Figure 3,
 316 and the relevant statistics in Table S2. We note here that, for the possible available observations per location, for
 317 the month of March there were slightly less available pixels for year 2020 than 2019, on average ~-15% and range
 318 between -5% and -22%, with the highest difference for Thessaloniki which was overcast the entire final week of
 319 March 2020 as already discussed. For April, slightly more pixels are available for year 2020, on average +5% and
 320 range between 1% and 11%.
 321



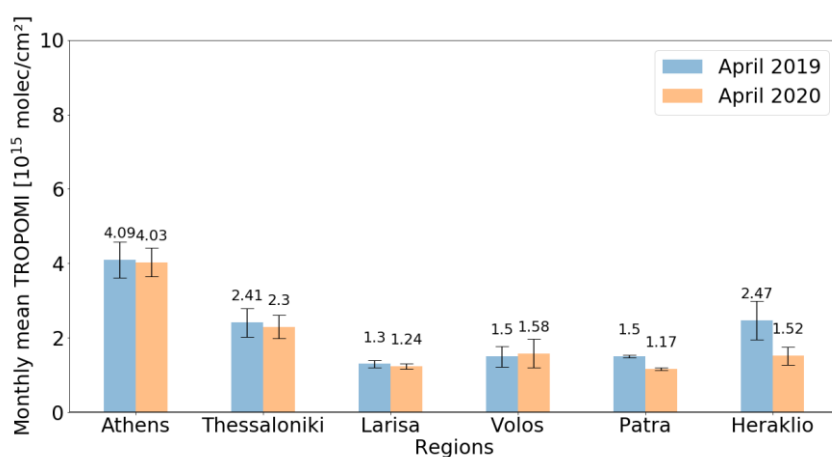


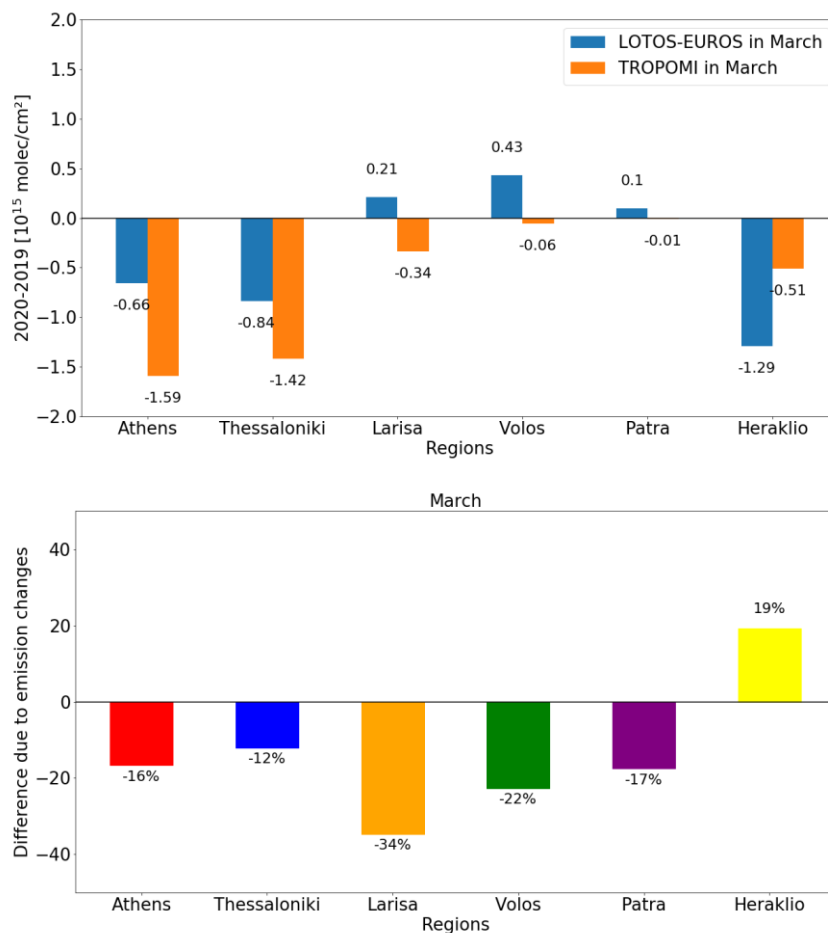
Figure 3. Monthly mean TROPOMI tropospheric NO₂ columns, in 10¹⁵ molecules/cm², for March [upper] and April [lower] for the 2019 [blue] and 2020 [orange] for the five major cities in Greece, from left to right, Athens, Thessaloniki, Larisa, Volos, Patra and Heraklio.

Table 1. Monthly mean TROPOMI NO₂ levels [10¹⁵ molecules/cm²] over major cities in Greece for March [left block] and April [right block] for year 2019 and 2020 and their relative difference, standard deviation and number of pixels [in brackets].

Location	03.2019	03.2020	% diff	04.2019	04.2020	% diff
Athens [12]	6.04±1.65	4.45±0.76	-26%	4.09±0.49	4.03±0.38	-1%
Thessaloniki [6]	4.13±0.34	2.71±0.38	-34%	2.41±0.28	2.30±0.22	-5%
Larisa [16]	1.72±0.22	1.38±0.17	-19%	1.30±0.13	1.24±0.09	-5%
Volos [3]	1.84±0.13	1.78±0.21	-3%	1.50±0.14	1.58±0.19	+5%
Patra [2]	1.30±0.10	1.42±0.19	+20%	1.50±0.02	1.17±0.01	-18%
Heraklio [4]	1.94±0.29	1.43±0.08	-26%	2.47±0.30	1.52±0.14	-39%

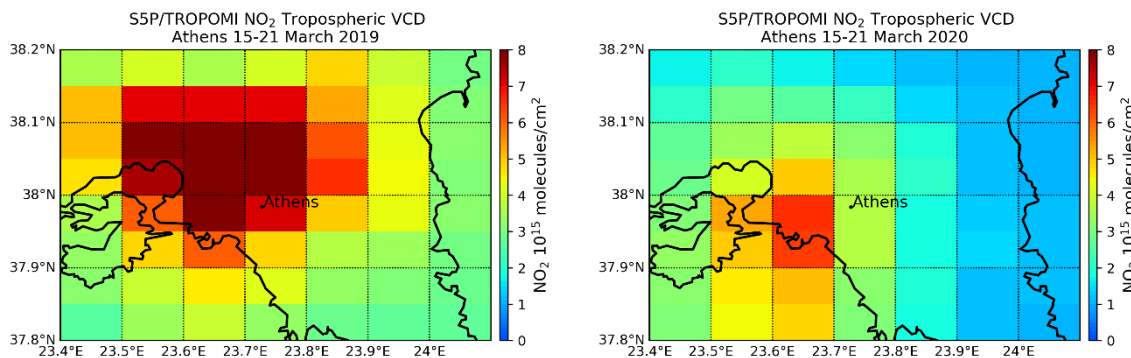
In Figure 4, upper, the monthly mean absolute differences in tropospheric NO₂ columns (10¹⁵ molecules/cm²) between 2020 and 2019 are shown for TROPOMI [orange] and LOTOS-EUROS [blue] for the six major cities in Greece, for Athens, Thessaloniki, Larisa, Volos, Patra and Heraklio. We opted to show absolute differences here, and not percentage ones as might be expected, since a small relative change on a low NO₂ abundance would result in the erroneous message of a large reduction, as was already shown in Figure 3. In the lower panel of Figure 4, the emission changes are quantified in the following manner: the percentage differences for LOTOS-EUROS between 2019 and 2020 are calculated, as the equivalent ones seen by TROPOMI. By subtracting the two percentage differences, and not directly comparing the two, the actual NO₂ emission reduction may be quantified.

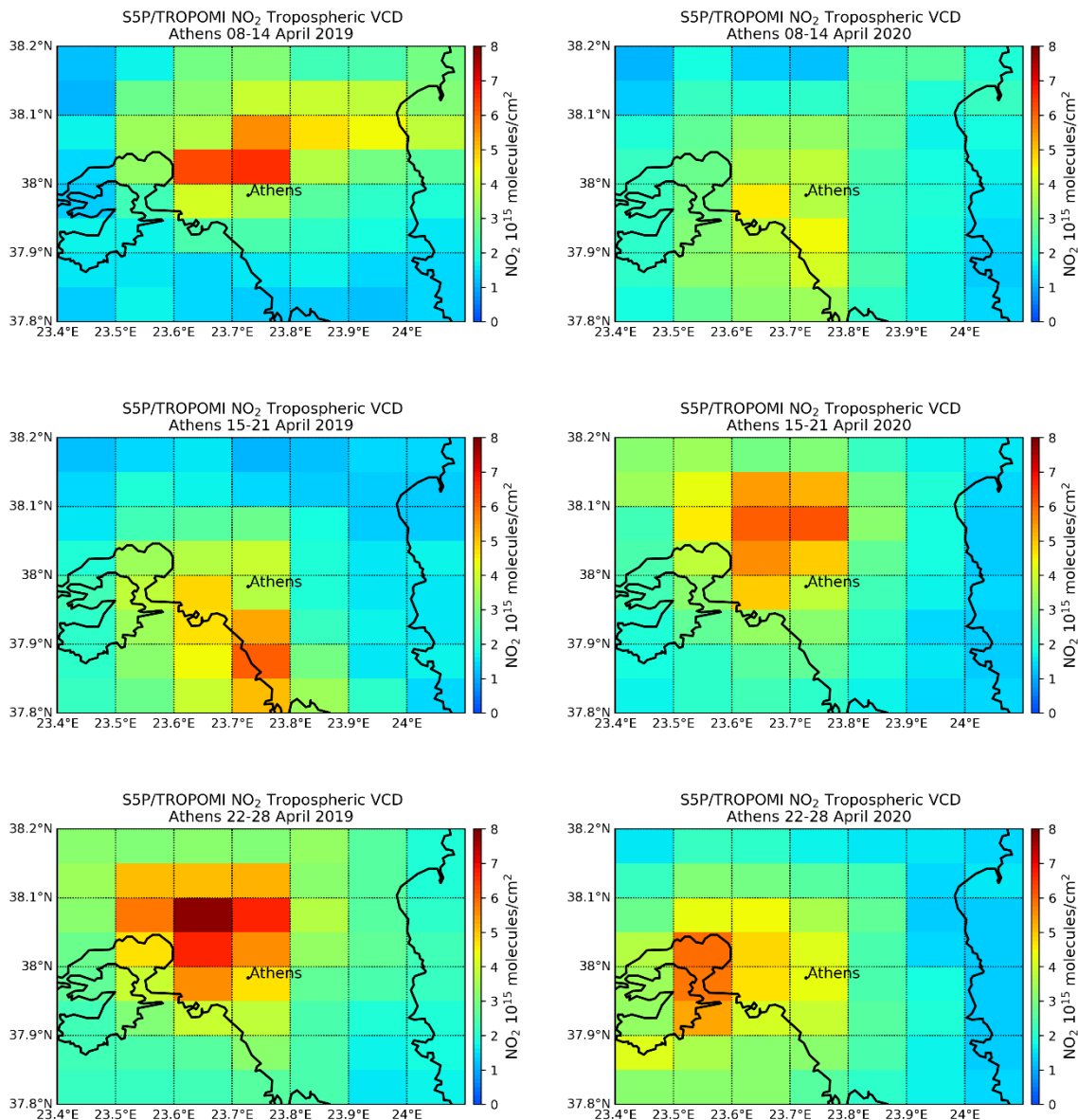
This percentage difference is found to be -16% for Athens, -12% for Thessaloniki, -34% for Larisa, -22% for Volos, -17% for Patra and +19%, for Heraklio. This study shows that, for relatively low tropospheric NO₂ columns of the order of 1.5x10¹⁵ molecules/cm² this methodology which is based on differences, may result in unexpected numerical findings. Similar studies which have examined the effects of the COVID-19 lockdown on air quality based on satellite observations have focused on Eastern China, on specific US and Canadian locations, as well as over the Po Valley in Italy, which observe orders of magnitude higher tropospheric NO₂ columns even for the reduced emissions period. As a result, our main tentative finding is that over Greece, a ~-10% reduction in tropospheric NO₂ columns as sensed by the S5P/TROPOMI instrument may be attributed to the reduced emissions due to the COVID-19 pandemic. We hence continue this study focusing only over the location with the highest observed tropospheric NO₂ columns, the capital city of Athens, in a weekly temporal scale, so as to possible refine this estimate.



348 Figure 4. Upper. Monthly mean absolute differences in tropospheric NO₂ columns (10¹⁵ molecules/cm²) between 2020 and 2019 are shown for
 349 TROPOMI [orange] and LOTOS-EUROS [blue] for the five major cities in Greece, from left to right, Athens, Thessaloniki, Larisa, Volos, Patra
 350 and Heraklio. Lower. The percentage differences that may be attributable to emission changes.

351 **3.2. Lockdown effects on weekly NO₂ levels over Athens**





352 Figure 5. Weekly mean TROPOMI tropospheric NO₂ columns, in 10¹⁵ molecules/cm², over Athens for 2019 [left] and 2020 [right]. First row, 15-
 353 21 March 2019; second, 8-14 April, third, 15-21 April and fourth, 22-28 April.

354 Without disregarding the possible contribution of central heating to total NO_x emissions, the largest decrease
 355 due to the COVID-19 lockdown is indeed observed over the main Greek hotspot, the city of Athens and its
 356 surroundings. In Figure 5, weekly mean TROPOMI tropospheric NO₂ columns, in 10¹⁵ molecules/cm², over Athens
 357 for 2019 [left] and 2020 [right] are shown for weeks 15-21 March (first row), 8-14 April (second row), 15-21 April
 358 (third row) and 22-28 April (fourth row). Apart from the obvious reduction in magnitude during the lockdown
 359 months, what is most prominent in this composite is the effect of the winds for both the location of the local
 360 maximum as well as the spread of the pollution plume, which further strengthens our decision not to perform one-
 361 on-one comparisons between the different NO₂ fields. In numbers, the average weekly NO₂ load over Athens
 362 sensed by TROPOMI is presented in Figure 6 where the 2019 averages are shown in blue and the 2020 ones in
 363 orange for weeks of March and April. Out of the 12 pixels considered for this sub-domain, which may provide up
 364 to 84 measurements for each week in the case of clear skies, for year 2019 an average of 53±16 [median of 52] clear
 365 sky S5P/TROPOMI observations were found whereas for year 2020 an average of 52±25 [median of 56]. Even

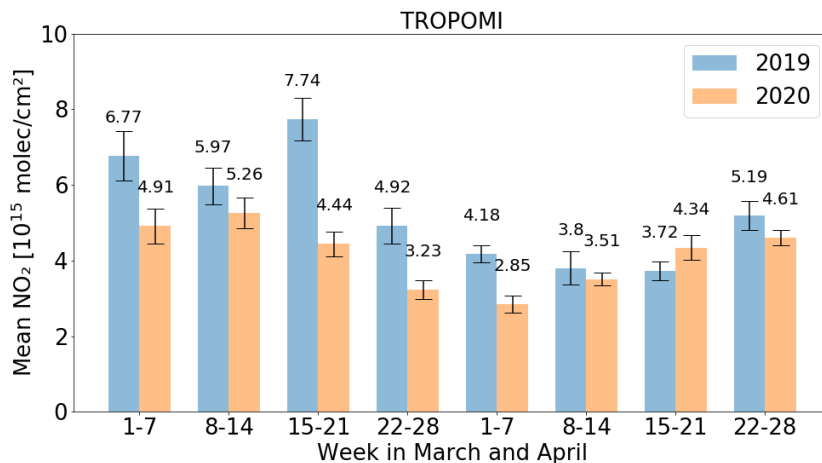
366 though the representativeness of the weekly levels can by no means be considered equal between the years, apart
367 from the penultimate week, TROPOMI reports lower NO₂ columns ranging between -8% to -43%. The MAXDOAS
368 observations over Athens also show a very similar behavior, reporting $6.77 \pm 6.85 \times 10^{15}$ and $3.60 \pm 1.83 \times 10^{15}$
369 molecules/cm² for March and April 2019, and 2.76 ± 3.17 and $2.77 \pm 2.44 \times 10^{15}$ molecules/cm² for March and April 2020
370 respectively, showing a much larger reduction for the month of March than the month of April.

371 The meteorology over these eight weeks over Athens shows that, temperature-wise, in 2019, the entire month
372 of March as well as the first three weeks of April, had very similar levels with a very hot spell affecting the last
373 week of April 2019 which was also Easter Week in Greece. In 2020, a cold front appeared during the third week of
374 March which lasted until mid-April when warmer weather appeared and remained (Figure S5). The mean vector
375 wind speed and direction, overlain as arrows in Figure S5, is very similar with mostly predominant northern winds
376 and very few cases of southerly winds. In the equivalent rose diagrams, Figure S6, we note again that the main
377 wind directions appear similar between the two periods [2019 in the left and 2020 in the right column] apart from
378 the last week of April [bottom row] were indeed the two weeks had very different directions, for the same
379 magnitude. Note that the percentiles are not constant between rose diagrams.

380 A question that often arises when examining a relatively short time period of a highly varying atmospheric
381 species is whether the period considered as “normal” was indeed normal from a climatological point of view. We
382 have opted to create a climatological mean based on the daily OMI/Aura NO₂ cloud-screened tropospheric column
383 L3 global gridded 0.25x0.25° v003 product (Krotkov et al., 2017; 2019) accessed from the NASA EarthData Giovanni
384 repository. The monthly variability of the tropospheric NO₂ load over Athens for year 2019, in blue, and 2020, in
385 orange, is shown in Figure 7, upper panel, as the percentage difference from the climatological mean (grey shaded
386 area). As is also observed by the TROPOMI instrument, the OMI observations also reveal a higher decrease for
387 March 2020 compared to March 2019, than the equivalent decrease for the April months. In Figure 7, lower panel,
388 the weekly variability of the tropospheric NO₂ load over Athens for year 2019, in blue, and 2020, in orange, is
389 shown, starting in week 1, the first week of March and covering eight weeks. In this representation as well, it is
390 shown that the weeks of March of 2020 were further from the climatological mean compared to the April 2020
391 ones, while the April 2019 weeks show overall lower NO₂ loads, as also shown by TROPOMI (Figure 6).

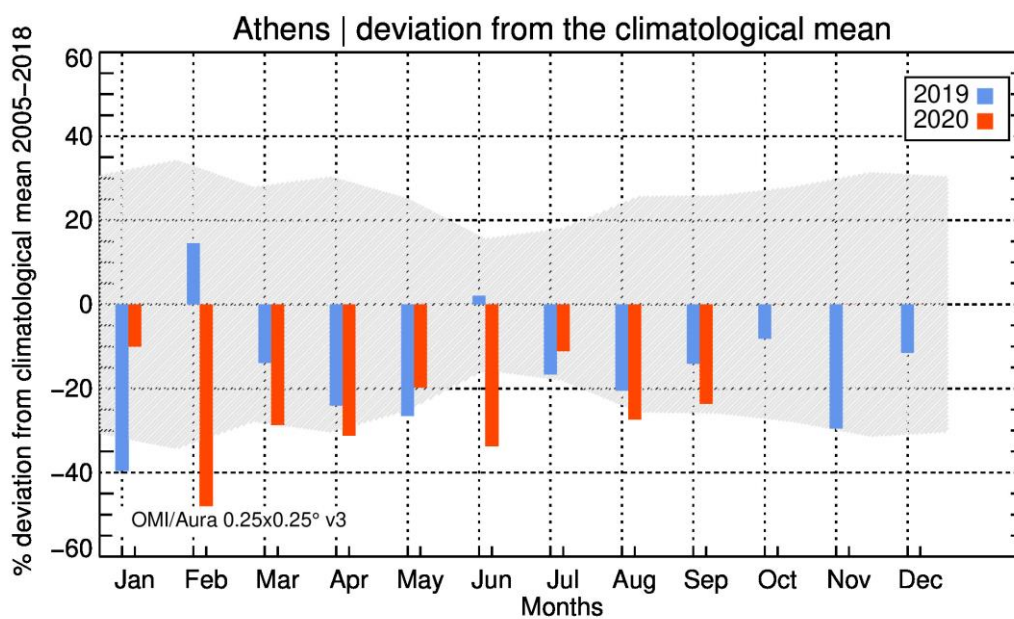
392 Another question that is also often discussed when examining such abrupt changes in localized emission sources
393 is whether in situ surface measurements depict the changes in the same order and magnitude. For the case of the
394 COVID-19 pandemic, a number of studies for European locations have appeared with surprising findings; in
395 Ropkins and Tate, 2021, measurements from automated monitoring stations across the UK showed abrupt NO₂
396 decreases at the onset of the UK lockdown, between ~25 to 50% at urban traffic and urban background stations.
397 Surprisingly, after the initial abrupt reduction, gradual increases were then observed through the rest of the UK
398 lockdown period. A similar finding is reported by Dakre, Mortimer and Neal, 2020, who show that the in situ air
399 quality stations in the north and middle of England measure a decrease in NO₂ concentrations in the lockdown
400 period of 17/03/20 – 30/04/20 whereas stations in the south of England measured an increase in NO₂ concentrations.
401 Putaud et al., 2020, studied in situ concentrations from an urban background and a regional background station in
402 the North of Italy and showed that that NO₂ concentrations decreased as a consequence of the lockdown by -30%
403 and -40% on average, respectively.

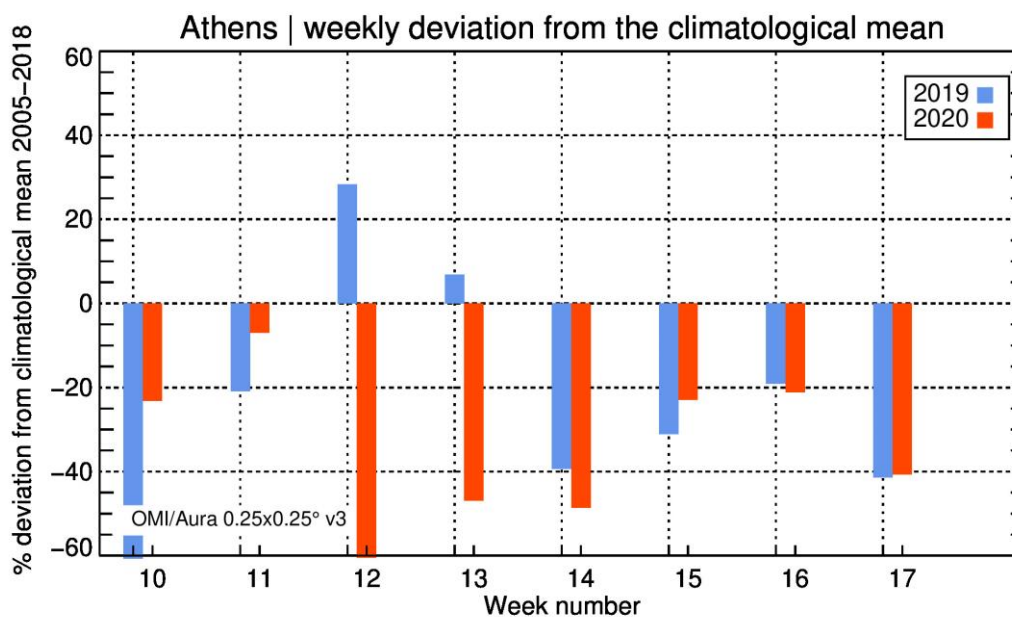
404



405 Figure 6. Weekly mean TROPOMI tropospheric NO₂ columns, in 10¹⁵ molecules/cm², for weeks in the 2019 [blue] and 2020 [orange] for Athens.

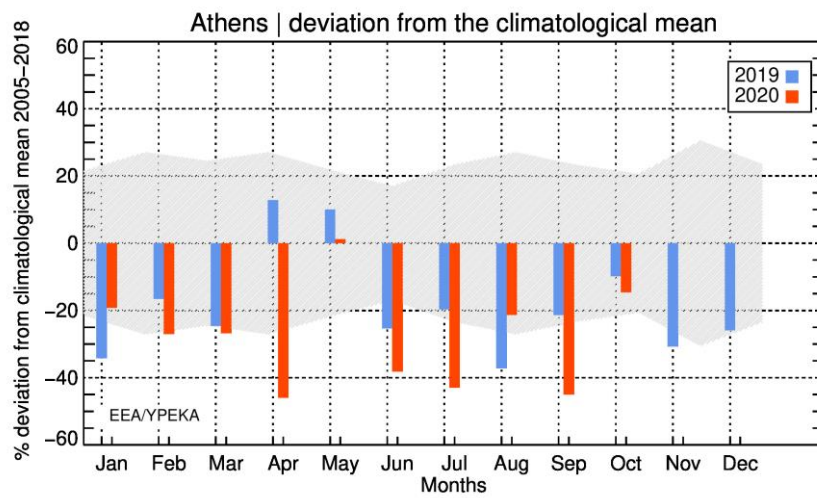
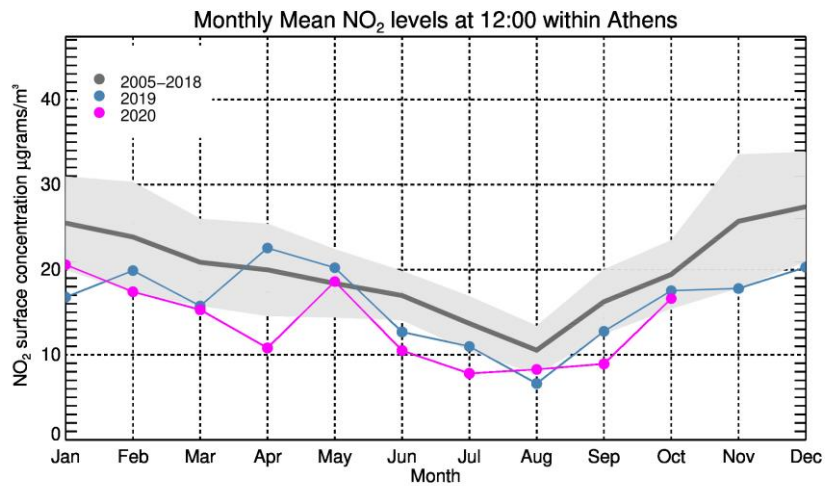
406
407





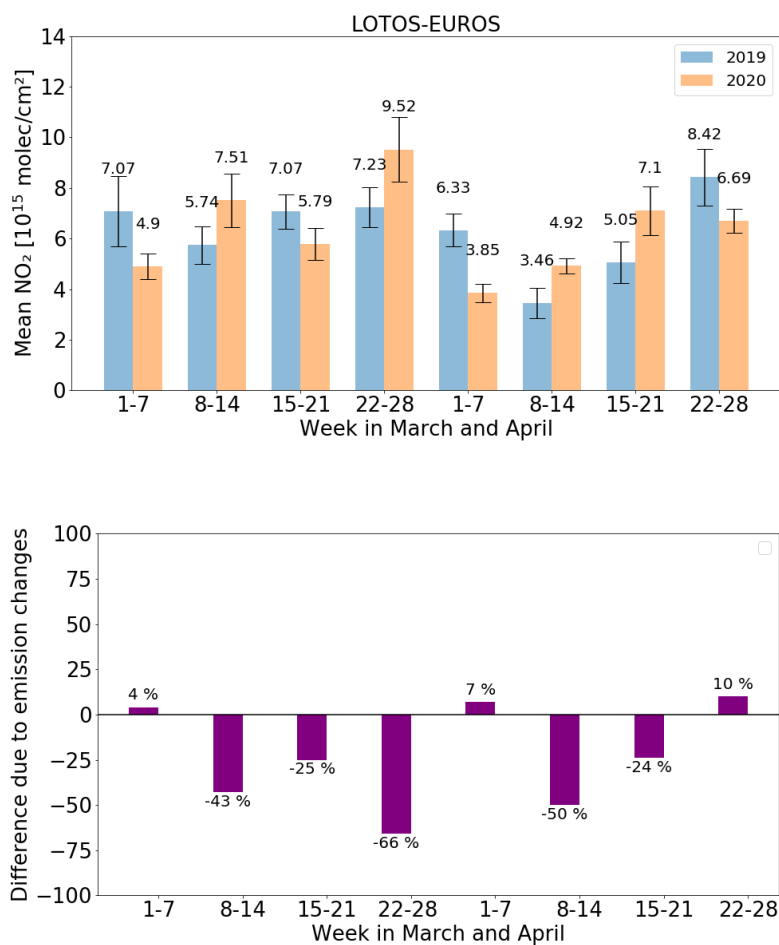
408 Figure 7. Upper. The OMI/Aura v003 L3 gridded cloud-screened tropospheric NO₂ monthly deviations from the climatological mean (grey
 409 shaded area) for year 2019 (in blue) and year 2020 (in orange.) Lower. The OMI/Aura v003 L3 gridded cloud-screened tropospheric NO₂ weekly
 410 deviations from the climatological mean for year 2019 (in blue) and year 2020 (in orange) starting in week 10, the first week of March.

411 For the purposes of this discussion we have analyzed the in situ surface NO₂ measurements reported by seven air
 412 quality stations around Athens, with their locations shown in Figure S3, and their individual monthly mean
 413 variability for 12:00 UTC is shown in Figure S4. These long-term observations are maintained by the Greek Ministry
 414 Environment & Energy, YPEKA, network who further report them to the European Environmental Agency, EEA,
 415 and are officially designated as industrial, urban and suburban locations. The measurement time closest to the
 416 TROPOMI overpass time over Athens was chosen to calculate a climatology between years 2005 and 2018, and in
 417 Figure 8, upper, the monthly mean NO₂ levels calculated from the time series shown in Figure S4, is presented The
 418 grey line and shaded area show the seasonal variability of the mean surface concentrations, in μgrams/m³, with
 419 higher levels during wintertime months and lower during summertime. Similar NO₂ concentrations are reported
 420 for both months of March 2019 (in blue) and 2020 (in purple), at the lower statistical level, while an unexpected
 421 increase for April (and May) 2019 show large differences to the lows found in April 2020, the full COVID lockdown
 422 month for Greece. This finding is clearer in the Figure 8, lower panel, where the monthly deviation of year 2019 (in
 423 blue) and year 2020 (in orange) are given as bars, overlaid against the grey shaded area which shows the variability
 424 of the climatological means. Contrary hence to what the space-born observations by both TROPOMI and OMI as
 425 well as the ground-based MAXDAS measurements show, the in situ measurements report a similar difference
 426 similar difference to the climatological mean for the months of March while April 2019 appears in the positive
 427 range, while April 2020 beyond the lower statistical level. Grivas et al., 2020, compared climatological hourly NO₂
 428 concentrations measured by an urban background station in the Athens basin (not included in our work) for years
 429 2016-2020 to days corresponding to the pre-lockdown (March 1-22), lockdown (March 23 – May 10) and post
 430 lockdown (May 11-31) periods of 2020. Overall, they report -6%, -41.5% and +8.7% between the periods of year
 431 2020 to the 2016-2020 equivalent.
 432



433 Figure 8. Upper. Monthly mean NO₂ surface concentrations, in µgrams/m³, for the climatological mean of 2005 to 2018 shown
 434 as a dark grey line and standard deviation (grey shaded area), year 2019 (in blue) and year 2020 (in purple) calculated from the
 435 levels reported by seven air quality stations, as shown in Figure S4. Lower. The monthly percentage deviation from the
 436 climatological mean (shaded grey area) for the months of 2019 in blue and 2020 in orange.

437



438 Figure 9. Upper. Weekly mean LOTOS-EUROS tropospheric NO₂ columns, in 10¹⁵ molecules/cm², for weeks in the 2019 [blue] and 2020 [orange]
 439 for Athens. Lower. The percentage differences attributed to emission changes, revealing the actual magnitude of the NO_x emissions decrease.

440 The contribution of the meteorological factors to the observed tropospheric NO₂ load can be assessed by the
 441 equivalent LOTOS-EUROS weekly averages, shown in the upper panel of Figure 9. As for Figure 4, bottom, the
 442 percentage difference of the LOTOS-EUROS simulations between 2019 and 2020 are calculated, as were those for
 443 the TROPOMI equivalent weekly means (Figure 6). The difference between those two relative differences is given
 444 in the lower panel of Figure 9. The fact that the CTM predicted an increase in NO₂ production for most weeks,
 445 under the assumption that the primary emissions remained stable between the two years, results in higher
 446 reduction levels ranging between -24% and -66% for 5 of the 8 weeks studied, while an assumed increase in
 447 emissions is calculated for the remaining 3 weeks with levels between +4 and +10%. These increases in emission
 448 levels, which are not corroborated by the in situ observations, give us an estimate on the uncertainty of this
 449 methodology, at ~10%. Even so, the average difference in emissions over Athens for these eight weeks is calculated
 450 at ~-20% from the S5P/TROPOMI tropospheric NO₂ observations.

452 4. Conclusions

453 In this work, Sentinel-5P/TROPOMI tropospheric NO₂ observations were studied in order to examine the
 454 possible positive effect on Greek air quality caused the recent COVID-19 pandemic lockdown. The country
 455 enforced severe movement restrictions and entire economic sectors gradually were shut down, starting from the

456 last weekend of February and gradually, activity per activity, reaching a total lockdown in effect from Monday 23rd
457 up to May 4th. The time period between March and April 2020, and the equivalent weeks in 2019, were analyzed
458 and compared for six, largest in population, cities in Greece on a monthly basis. TROPOMI monthly mean
459 tropospheric nitrogen dioxide, NO₂, observations showed a change of between -34% and +20% [-39% to +5%] with
460 an average of -15% [-11%] for March and April 2020 respectively, compared to the previous year, for the urban
461 areas, attributable mostly to vehicular emission reductions. For the capital city of Athens, weekly reductions in the
462 TROPOMI tropospheric NO₂ columns, between -8% and -43%, for the seven of the eight weeks studied were found,
463 corroborated by the space-born OMI/Aura observations as well as ground-based Multi-Axis Differential Optical
464 Absorption Spectroscopy, MAXDOAS, measurements. Stronger reductions were reported by seven in situ air
465 quality stations in Athens that reported measurements to the European Environmental Agency Air Quality
466 database, with monthly decreases reaching -40% for the month of April 2020. In order to eliminate the expected
467 meteorological effects on the observed NO₂ levels, Chemical Transport Modelling simulations, provided by the
468 LOTOS-EUROS CTM, show that the magnitude of these satellite-sensed reductions cannot solely be attributed to
469 the difference in meteorological factors affecting NO₂ levels during March and April 2020 and the equivalent time
470 periods of the previous year. Taking this factor into account, the resulting decline due to the COVID-19 related
471 measures was estimated to range between -10% and -20% for the different spatiotemporal scales studied in this
472 work, taking into account possible uncertainties of the methodology considering the low tropospheric NO₂ levels
473 observed around Greece.

474 **Author Contributions:** The data analysis was performed by I.S., A.K. and M.E.K.; methodology and conceptualization by D.S.
475 and I.P.; software development by I.S. and A.K.; writing—original draft preparation by M.E.K.; review and editing by D.S.,
476 A.S., A.M., J.v.G. and H.E. All authors have read and agreed to the published version of the manuscript.

477 **Funding:** This research has been co-financed by the European Union (European Regional Development Fund) and Greek
478 national funds through the Operational Program “Competitiveness, Entrepreneurship and Innovation” (NSRF 2014-2020) by
479 the “Panhellenic Infrastructure for Atmospheric Composition and Climate Change” project (MIS 5021516) and well as the
480 “Innovative system for Air Quality Monitoring and Forecasting” project [code T1EDK-01697, MIS 5031298], implemented under
481 the Action “Reinforcement of the Research and Innovation” Infrastructure.

482 **Acknowledgments:** We acknowledge the usage of modified Copernicus Sentinel data 2019-2020. Results presented in this work
483 have been produced using the Aristotle University of Thessaloniki (AUTH) High Performance Computing Infrastructure and
484 Resources. M.E.K., I.S. and D.S. would like to acknowledge the support provided by the IT Center of the AUTH throughout the
485 progress of this research work. M.E.K. and A.K. would also like to acknowledge the support provided by the Atmospheric
486 Toolbox®.

487 **Conflicts of Interest:** The authors declare no conflict of interest.

488 **Data availability:** The S5P/TROPOMI data are publicly available via the Copernicus Open Data Access Hub,
489 <https://scihub.copernicus.eu/>. The LOTOS-EUROS simulations are available upon request. The air quality monitoring station
490 data are publicly available via the European Environmental Agency Air Quality monitoring service,
491 <https://discomap.eea.europa.eu/map/fme/AirQualityExport.htm> and the Greek Ministry Environment & Energy monitoring
492 network, <https://ypen.gov.gr/perivallon/poiotita-tis-atmosfairas/dedomena-metriseon-atmosfairikis-rypansis/>. The OMI/Aura
493 NO₂ cloud-screened tropospheric column L3 global gridded 0.25x0.25° v003 product are publicly available from the NASA
494 EarthData Giovanni repository, <https://giovanni.gsfc.nasa.gov/giovanni/>. The MAXDOAS observations discussed in this text
495 are publicly available from <https://mpc-vdaf-server.tropomi.eu/no2/no2-offl-maxdoas/athens>.

496 References

- 497 Bauwens, M., Compornolle, S., Stavrou, T., Müller, J.-F., van Gent, J., Eskes, H., et al. (2020) Impact of coronavirus outbreak
498 on NO₂ pollution assessed using TROPOMI and OMI observations. *Geophysical Research Letters*, 47,
499 e2020GL087978. <https://doi.org/10.1029/2020GL087978>
- 500 Beirle, S., Boersma, K. F., Platt, U., Lawrence, M. G., and Wagner, T. (2011). Megacity emissions and lifetimes of nitrogen oxides
501 probed from space. *Science*, 333:1737–1739, DOI: 10.1126/science.1207824.
- 502 Schaub, D., Brunner, D., Boersma, K. F., Keller, J., Folini, D., Buchmann, B., Berresheim, H., and Staehelin, J.: SCIAMACHY
503 tropospheric NO₂ over Switzerland: estimates of NO_x lifetimes and impact of the complex Alpine topography on the retrieval,
504 *Atmos. Chem. Phys.*, 7, 5971–5987, <https://doi.org/10.5194/acp-7-5971-2007>, 2007.

505 Blechschmidt, A.-M., Arteta, J., Coman, A., Curier, L., Eskes, H., Foret, G., Gielen, C., Hendrick, F., Marécal, V., Meleux, F.,
506 Parmentier, J., Peters, E., Pinardi, G., Pitters, A. J. M., Plu, M., Richter, A., Segers, A., Sofiev, M., Valdebenito, Á. M., Van
507 Roozendaal, M., Vira, J., Vlemmix, T., and Burrows, J. P.: Comparison of tropospheric NO₂ columns from MAX-DOAS retrievals
508 and regional air quality model simulations, *Atmos. Chem. Phys.*, 20, 2795–2823, <https://doi.org/10.5194/acp-20-2795-2020>, 2020.
509 Boersma, K. F., Eskes, H. J., Dirksen, R. J., van der A, R. J., Veeffkind, J. P., Stammes, P., Huijnen, V., Kleipool, Q. L., Sneep, M.,
510 Claas, J., Leitão, J., Richter, A., Zhou, Y., and Brunner, D.: An improved tropospheric NO₂ column retrieval algorithm for the
511 Ozone Monitoring Instrument, *Atmos. Meas. Tech.*, 4, 1905–1928, <https://doi.org/10.5194/amt-4-1905-2011>, 2011.
512 Boersma, K. F., Eskes, H. J., Richter, A., De Smedt, I., Lorente, A., Beirle, S., van Geffen, J. H. G. M., Zara, M., Peters, E., Van
513 Roozendaal, M., Wagner, T., Maasakkers, J. D., van der A, R. J., Nightingale, J., De Rudder, A., Irie, H., Pinardi, G., Lambert, J.-
514 C., and Compernelle, S. C.: Improving algorithms and uncertainty estimates for satellite NO₂ retrievals: results from the quality
515 assurance for the essential climate variables (QA4ECV) project, *Atmos. Meas. Tech.*, 11, 6651–6678, [https://doi.org/10.5194/amt-](https://doi.org/10.5194/amt-11-6651-2018)
516 [11-6651-2018](https://doi.org/10.5194/amt-11-6651-2018), 2018.
517 Castellanos, P., Boersma, K. Reductions in nitrogen oxides over Europe driven by environmental policy and economic recession.
518 *Sci Rep* 2, 265 (2012). <https://doi.org/10.1038/srep00265>
519 Cersosimo, A.; Serio, C.; Masiello, G. TROPOMI NO₂ Tropospheric Column Data: Regridding to 1 km Grid-Resolution and
520 Assessment of their Consistency with In Situ Surface Observations. *Remote Sens.*, 12, <https://doi.org/10.3390/rs12142212> 2020.
521 Curier, R. L., R. Kranenburg, A.J.S. Segers, R.M.A. Timmermans, M. Schaap, Synergistic use of OMI NO₂ tropospheric columns
522 and LOTOS-EUROS to evaluate the NO_x emission trends across Europe, *Remote Sensing of Environment*, 149, 2014, 58–69,
523 <https://doi.org/10.1016/j.rse.2014.03.032>.
524 Curier, R. L., R. Timmermans, S. Calabretta-Jongen, H. Eskes, A. Segers, D. Swart, M. Schaap, Improving ozone forecasts over
525 Europe by synergistic use of the LOTOS-EUROS chemical transport model and in-situ measurements, *Atmospheric*
526 *Environment*, 60, 2012, 217–226, <https://doi.org/10.1016/j.atmosenv.2012.06.017>.
527 Dacre, H. F., A H Mortimer and L S Neal, How have surface NO₂ concentrations changed as a result of the UK's COVID-19
528 travel restrictions? *Environmental Research Letters*, 15, 10, <https://iopscience.iop.org/article/10.1088/1748-9326/abb6a2>, 2020.
529 Daniel J. Jacob and Darrell A. Winner, Effect of climate change on air quality, *Atmospheric Environment*, Volume 43, Issue 1,
530 Pages 51-63, <https://doi.org/10.1016/j.atmosenv.2008.09.051>, 2009.
531 Ding, J., van der A, R. J., Eskes, H. J., Mijling, B., Stavrakou, T., van Geffen, J. H. G. M., et al. (2020). NO_x emissions reduction
532 and rebound in China due to the COVID-19 crisis. *Geophysical Research Letters*, 46, e2020GL089912.
533 <https://doi.org/10.1029/2020GL089912>
534 Ding, J., van der A, R. J., Mijling, B., Levelt, P. F., and Hao, N.: NO_x emission estimates during the 2014 Youth Olympic Games
535 in Nanjing, *Atmos. Chem. Phys.*, 15, 9399–9412, <https://doi.org/10.5194/acp-15-9399-2015>, 2015. Eskes, H. J. and Boersma, K. F.:
536 Averaging kernels for DOAS total-column satellite retrievals, *Atmos. Chem. Phys.*, 3(5), 1285–1291, doi:10.5194/acp-3-1285-
537 2003, 2003.
538 European Environmental Agency, EEA: Air quality in Europe – 2019 report, doi:10.2800/822355, available at:
539 <https://www.eea.europa.eu/publications/air-quality-in-europe-2019>, last access: 29.04.2020.
540 European Environmental Agency, EEA: Report No 8/2019, European Union emission inventory report 1990-2017 under the
541 UNECE Convention on Long-range Transboundary Air Pollution (LRTAP), doi:10.2800/78220, available at:
542 <https://www.eea.europa.eu/publications/european-union-emissions-inventory-report-2017>, last access: 29.04.2020
543 European Union, EU: The Environmental Implementation Review 2019, COUNTRY REPORT: GREECE, available at
544 https://ec.europa.eu/environment/eir/pdf/report_el_en.pdf, last access: 30.04.2020
545 Fameli, K.M. and V.D. Assimakopoulos, Development of a road transport emission inventory for Greece and the Greater Athens
546 Area: Effects of important parameters, *Science of The Total Environment*, 505, 2015, 770-786,
547 <https://doi.org/10.1016/j.scitotenv.2014.10.015>.
548 Fountoukis, C. and Nenes, A.: ISORROPIA II: a computationally efficient thermodynamic equilibrium model for K⁺-Ca²⁺-Mg²⁺-
549 NH₄⁺-Na⁺-SO₄²⁻-NO₃⁻-Cl⁻-H₂O aerosols, *Atmos. Chem. Phys.*, 7, 4639–4659, <https://doi.org/10.5194/acp-7-4639-2007>, 2007.
550 Georgoulias, A. K., van der A, R. J., Stammes, P., et al., Trends and trend reversal detection in 2 decades of tropospheric NO₂
551 satellite observations, *Atmos. Chem. Phys.*, 19, 6269–6294, <https://doi.org/10.5194/acp-19-6269-2019>, 2019.
552 Gery, M. W., Whitten, G. Z., Killus, J. P., and Dodge, M. C. (1989), A photochemical kinetics mechanism for urban and regional
553 scale computer modeling, *J. Geophys. Res.*, 94(D10), 12925– 12956, doi:10.1029/JD094iD10p12925.
554 Goldberg, D. L., Anenberg, S. C., Griffin, D., McLinden, C. A., Lu, Z., & Streets, D. G. (2020). Disentangling the impact of the
555 COVID-19 lockdowns on urban NO₂ from natural variability, *Geophysical Research Letters*, 47,
556 e2020GL089269. <https://doi.org/10.1029/2020GL089269>

557 Grivas, G.; Athanasopoulou, E.; Kakouri, A.; Bailey, J.; Liakakou, E.; Stavroulas, I.; Kalkavouras, P.; Bougiatioti, A.; Kaskaoutis,
558 D.G.; Ramonet, M.; Mihalopoulos, N.; Gerasopoulos, E. Integrating in situ Measurements and City Scale Modelling to Assess
559 the COVID-19 Lockdown Effects on Emissions and Air Quality in Athens, Greece. *Atmosphere* 2020, 11, 1174.

560 HAS: Hellenic Statistical Authority, 2011 Population-Housing Census, 2011, available at [https://www.statistics.gr/2011-census-](https://www.statistics.gr/2011-census-pop-hous)
561 [pop-hous](https://www.statistics.gr/2011-census-pop-hous), last access: 07.12.2020.

562 HAS: Hellenic Statistical Authority, Air Emission Accounts, 2017, available at [https://www.statistics.gr/en/statistics/-](https://www.statistics.gr/en/statistics/-/publication/SOP08/)
563 [/publication/SOP08/](https://www.statistics.gr/en/statistics/-/publication/SOP08/), last access: 07.02.2020.

564 Ialongo, I., Virta, H., Eskes, H., Hovila, J., and Douros, J.: Comparison of TROPOMI/Sentinel-5 Precursor NO₂ observations with
565 ground-based measurements in Helsinki, *Atmos. Meas. Tech.*, 13, 205–218, <https://doi.org/10.5194/amt-13-205-2020>, 2020.

566 IPTO: Independent Power Transmission Operator, Monthly Energy Reports, 2020,
567 <https://www.admie.gr/en/market/reports/monthly-energy-balance>, last access: 07.02.2020

568 Marécal, V., Peuch, V.-H., Andersson, C., Andersson, S., Arteta, J., Beekmann, M., Benedictow, A., Bergström, R., Bessagnet, B.,
569 Cansado, A., Chéroux, F., Colette, A., Coman, A., Curier, R. L., Denier van der Gon, H. A. C., Drouin, A., Elbern, H., Emili, E.,
570 Engelen, R. J., Eskes, H. J., Foret, G., Friese, E., Gauss, M., Giannaros, C., Guth, J., Joly, M., Jaumouillé, E., Josse, B., Kadyrov,
571 N., Kaiser, J. W., Krajsek, K., Kuenen, J., Kumar, U., Liora, N., Lopez, E., Malherbe, L., Martinez, I., Melas, D., Meleux, F., Menut,
572 L., Moinat, P., Morales, T., Parmentier, J., Piacentini, A., Plu, M., Poupkou, A., Queguiner, S., Robertson, L., Rouil, L., Schaap,
573 M., Segers, A., Sofiev, M., Tarasson, L., Thomas, M., Timmermans, R., Valdebenito, Á., van Velthoven, P., van Versendaal, R.,
574 Vira, J., and Ung, A.: A regional air quality forecasting system over Europe: the MACC-II daily ensemble production, *Geosci.*
575 *Model Dev.*, 8, 2777–2813, <https://doi.org/10.5194/gmd-8-2777-2015>, 2015.

576 Jacob, D. J. (1999). *Introduction to Atmospheric Chemistry*. Princeton University Press, ISBN-10: 0691001855.

577 Krotkov, N. A., Lamsal, L. N., Celarier, E. A., Swartz, W. H., Marchenko, S. V., Bucsela, E. J., Chan, K. L., Wenig, M., and Zara,
578 M.: The version 3 OMI NO₂ standard product, *Atmos. Meas. Tech.*, 10, 3133–3149, <https://doi.org/10.5194/amt-10-3133-2017>,
579 2017.

580 Krotkov, Nikolay, Lok N. Lamsal, Sergey V. Marchenko, Edward A. Celarier, Eric J. Bucsela, William H. Swartz, Joanna Joiner
581 and the OMI core team (2019), OMI/Aura NO₂ Cloud-Screened Total and Tropospheric Column L3 Global Gridded 0.25 degree
582 x 0.25 degree V3, NASA Goddard Space Flight Center, Goddard Earth Sciences Data and Information Services Center (GES
583 DISC), Accessed: [09.12.2020], 10.5067/Aura/OMI/DATA3007

584 Kuenen, J. J. P., Visschedijk, A. J. H., Jozwicka, M., and Denier van der Gon, H. A. C.: TNO-MACC_II emission inventory; a
585 multi-year (2003–2009) consistent high-resolution European emission inventory for air quality modelling, *Atmos. Chem. Phys.*,
586 14, 10963–10976, <https://doi.org/10.5194/acp-14-10963-2014>, 2014.

587 Lamsal, L. N., Martin, R. V., van Donkelaar, A., Celarier, E. A., Bucsela, E. J., Boersma, K. F., Dirksen, R., Luo, C., and Wang,
588 Y. (2010), Indirect validation of tropospheric nitrogen dioxide retrieved from the OMI satellite instrument: Insight into the
589 seasonal variation of nitrogen oxides at northern midlatitudes, *J. Geophys. Res.*, 115, D05302, doi:10.1029/2009JD013351.

590 Liu, Fei, Aaron Page, Sarah A. Strobe, Yasuko Yoshida, Sungyeon Choi, Bo Zheng, Lok N. Lamsal, Can Li, Nikolay A. Krotkov,
591 Henk Eskes, Ronald van der A, Pepijn Veeffkind, Pieternel Levelt, Joanna Joiner, Oliver P. Hauser, Abrupt declines in
592 tropospheric nitrogen dioxide over China after the outbreak of COVID-19, *Science Advances*, 6, 28,
593 <https://doi.org/10.1126/sciadv.abc2992>, 2020.

594 Lorente, A., Boersma, K.F., Eskes, H.J. *et al.* Quantification of nitrogen oxides emissions from build-up of pollution over Paris
595 with TROPOMI. *Sci Rep* 9, 20033 (2019). <https://doi.org/10.1038/s41598-019-56428-5>.

596 Manders, A. M. M., Builtjes, P. J. H., Curier, L., Denier van der Gon, H. A. C., Hendriks, C., Jonkers, S., Kranenburg, R., Kuenen,
597 J. J. P., Segers, A. J., Timmermans, R. M. A., Visschedijk, A. J. H., Wichink Kruit, R. J., van Pul, W. A. J., Sauter, F. J., van der
598 Swaluw, E., Swart, D. P. J., Douros, J., Eskes, H., van Meijgaard, E., van Ulft, B., van Velthoven, P., Banzhaf, S., Mues, A. C.,
599 Stern, R., Fu, G., Lu, S., Heemink, A., van Velzen, N., and Schaap, M.: Curriculum vitae of the LOTOS-EUROS (v2.0) chemistry
600 transport model, *Geosci. Model Dev.*, 10, 4145–4173, <https://doi.org/10.5194/gmd-10-4145-2017>, 2017.

601 Mijling, B., and van der A, R. J. (2012), Using daily satellite observations to estimate emissions of short-lived air pollutants on a
602 mesoscopic scale, *J. Geophys. Res.*, 117, D17302, doi:10.1029/2012JD017817.

603 Mijling, B., R. van der A, K. Boersma, M. Van Roozendaal, I. De Smedt, and H. Kelder (2009). Reductions of NO₂ detected from
604 space during the 2008 Beijing Olympic Games. *Geophys. Res. Lett.* 36, L13801.

605 Miyazaki, K., Bowman, K., Sekiya, T., Jiang, Z., Chen, X., Eskes, H., et al. (2020). Air quality response in China linked to the 2019
606 novel coronavirus (COVID-19) lockdown. *Geophysical Research Letters*, 47, e2020GL089252.
607 <https://doi.org/10.1029/2020GL089252>

608 Putaud, J.-P., Pozzoli, L., Pisoni, E., Martins Dos Santos, S., Lagler, F., Lanzani, G., Dal Santo, U., and Colette, A.: Impacts of the
609 COVID-19 lockdown on air pollution at regional and urban background sites in northern Italy, *Atmos. Chem. Phys. Discuss.*,
610 <https://doi.org/10.5194/acp-2020-755>, in review, 2020.

611 ROCVR: Quarterly Validation Report of the Sentinel-5 Precursor Operational Data Products #08: April 2018 – August 2020, S5P
612 Mission Performance Centre Reference, S5P-MPC-IASB-ROCVR-08.01.01-20200921, #08, 08.01.01, [https://s5p-mpc-
614 vdaf.aeronomie.be/ProjectDir/reports/pdf/S5P-MPC-IASB-ROCVR-08.01.01-20200921_FINAL.pdf](https://s5p-mpc-
613 vdaf.aeronomie.be/ProjectDir/reports/pdf/S5P-MPC-IASB-ROCVR-08.01.01-20200921_FINAL.pdf), last accessed: 17.12.2020,
2020.

615 Ropkins, Karl and James E. Tate, Early observations on the impact of the COVID-19 lockdown on air quality trends across the
616 UK, *Science of The Total Environment*, 745, <https://doi.org/10.1016/j.scitotenv.2020.142374>, 2021

617 Schaap M, Kranenburg R, Curier L, Jozwicka M, Dammers E, Timmermans R. Assessing the Sensitivity of the OMI-NO₂ Product
618 to Emission Changes across Europe. *Remote Sensing*. 2013; 5(9):4187-4208, <https://doi.org/10.3390/rs5094187>

619 Skoulidou, I., Koukouli, M.-E., Manders, A., Segers, A., Karagkiozidis, D., Gratsea, M., Balis, D., Bais, A., Gerasopoulos, E.,
620 Stavrakou, T., van Geffen, J., Eskes, H., and Richter, A.: Evaluation of the LOTOS-EUROS NO₂ simulations using ground-based
621 measurements and S5P/TROPOMI observations over Greece, *Atmos. Chem. Phys. Discuss.*, [https://doi.org/10.5194/acp-2020-
987](https://doi.org/10.5194/acp-2020-
622 987), in review, 2020.

623 Seo, J., Kim, J. Y., Youn, D., Lee, J. Y., Kim, H., Lim, Y. B., Kim, Y., and Jin, H. C.: On the multiday haze in the Asian continental
624 outflow: the important role of synoptic conditions combined with regional and local sources, *Atmos. Chem. Phys.*, 17, 9311–
625 9332, <https://doi.org/10.5194/acp-17-9311-2017>, 2017.

626 Stavrakou, T., Müller, J.-F., Boersma, K. F., De Smedt, I., and van der A, R. J. (2008), Assessing the distribution and growth rates
627 of NO_x emission sources by inverting a 10-year record of NO₂ satellite columns, *Geophys. Res. Lett.*, 35, L10801,
628 doi:10.1029/2008GL033521.

629 van der A, R. J., Eskes, H. J., Boersma, K. F., van Noije, T. P. C., Van Roozendael, M., De Smedt, I., Peters, D. H. M. U., and
630 Meijer, E. W. (2008), Trends, seasonal variability and dominant NO_x source derived from a ten year record of NO₂ measured
631 from space, *J. Geophys. Res.*, 113, D04302, doi:10.1029/2007JD009021.

632 van Geffen, J. H. G. M., Eskes, H. J., Boersma, K. F., Maasackers J. D. and Veeffkind, J. P., TROPOMI ATBD of the total and
633 tropospheric NO₂ data products, Report S5P-KNMI-L2-0005-RP, version 1.4.0, released 6 Feb. 2019, KNMI, De Bilt, The
634 Netherlands, available at <http://www.tropomi.eu/documents/atbd/>, last access: 08 May 2020.

635 Veeffkind, J. P. et al. TROPOMI on the ESA Sentinel-5 Precursor: A GMES mission for global observations of the atmospheric
636 composition for climate, air quality and ozone layer applications. *Rem. Sens. Env.* 120, 70–83 (2012),
637 <https://doi.org/10.1016/j.rse.2011.09.027>.

638 Virghileanu, M.; Săvulescu, I.; Mihai, B.-A.; Nistor, C.; Dobre, R. Nitrogen Dioxide (NO₂) Pollution Monitoring with Sentinel-
639 5P Satellite Imagery over Europe during the Coronavirus Pandemic Outbreak. *Remote Sens.* 2020, 12,
640 <https://doi.org/10.3390/rs12213575>, 2020.

641 Vlemmix, T., Eskes, H. J., Piters, A. J. M., Schaap, M., Sauter, F. J., Kelder, H., and Levelt, P. F.: MAX-DOAS tropospheric nitrogen
642 dioxide column measurements compared with the Lotos-Euros air quality model, *Atmos. Chem. Phys.*, 15, 1313–1330,
643 <https://doi.org/10.5194/acp-15-1313-2015>, 2015.

644 Timmermans R., Eskes H., Builtjes P., Segers A., Swart D., Schaap M. (2011) LOTOS-EUROS Air Quality Forecasts by
645 Assimilation of OMI Tropospheric NO₂ Columns. In: Steyn D., Trini Castelli S. (eds) Air Pollution Modeling and its Application
646 XXI. NATO Science for Peace and Security Series C: Environmental Security. Springer, Dordrecht.

647 Vrekoussis, M., Richter, A., Hilboll, A., et al., Economic Crisis Detected from Space: Air Quality observations over
648 Athens/Greece, *Geophys. Res. Lett.*, 40, 458–463, <https://doi.org/10.1002/grl.50118>, 2013.

649 World Health Organization, WHO: Ambient air pollution: A global assessment of exposure and burden of disease, World
650 Health Organisation, ISBN: 9789241511353, Bonn, 2016.

651 Zyrichidou, I., D. Balis, M.E. Koukouli, et al., Adverse results of the economic crisis: A study on the emergence of enhanced
652 formaldehyde (HCHO) levels seen from satellites over Greek urban sites, *Atmospheric Research*,
653 <https://doi.org/10.1016/j.atmosres.2019.03.017>, 2019.

654



© 2020 by the authors. Submitted for possible open access publication under the terms
and conditions of the Creative Commons Attribution (CC BY) license
(<http://creativecommons.org/licenses/by/4.0/>).